Mineralogical Magazine, June 2014, Vol. 78(3), pp. 483–496

Kihlmanite-(Ce), $Ce_2TiO_2[SiO_4](HCO_3)_2(H_2O)$, a new rare-earth mineral from the pegmatites of the Khibiny alkaline massif, Kola Peninsula, Russia

V. N. Yakovenchuk[1,2], S. V. Krivovichev[1,3], G. Y. Ivanyuk[1,2,]*, Ya. A. Pakhomovsky[1,2], E. A. Selivanova[1,2], E. A. Zhitova[3], G. O. Kalashnikova[1], A. A. Zolotarev[3], J. A. Mikhailova[1,2] and G. I. Kadyrova[4]

[1] Nanomaterials Research Centre, Kola Science Centre of the Russian Academy of Sciences, 14 Fersman Street, Apatity 184200, Murmansk Region, Russia

[2] Geological Institute, Kola Science Centre of the Russian Academy of Sciences, 14 Fersman Street, Apatity 184200, Murmansk Region, Russia

[3] Department of Crystallography, St. Petersburg State University, University Emb. 7/9, St. Petersburg 199034, Russia

[4] Institute of Chemistry and Technology of Rare Elements and Mineral Resources, Kola Science Centre, Russian Academy of Sciences, 14 Fersman Street, Apatity 184200, Murmansk Region, Russia

[*Received 30 September 2013; Accepted 23 January 2014; Associate Editor: E. Grew*]

ABSTRACT

Kihlmanite-(Ce), $Ce_2TiO_2[SiO_4](HCO_3)_2(H_2O)$, is a new rare-earth titanosilicate carbonate, closely related to tundrite-(Ce). It is triclinic, $P\bar{1}$, a = 4.994(2), b = 7.54(2), c = 15.48(4) Å, α = 103.5(4), β = 90.7(2), γ = 109.2(2)°, V = 533(1) Å^3, Z = 2 (from powder diffraction data) or a = 5.009(5), b = 7.533(5), c = 15.407(5) Å, α = 103.061(5), β = 91.006(5), γ = 109.285(5)°, V = 531.8(7) Å^3, Z = 2 (from single-crystal X-ray diffraction data). The mineral was found in the arfvedsonite-aegirine-microcline vein in fenitized metavolcanic rock at the foot of the Mt Kihlman (Chil'man), near the western contact of the Devonian Khibiny alkaline massif and the Proterozoic Imandra-Varzuga greenstone belt. It forms brown spherulites (up to 2 cm diameter) and sheaf-like aggregates of prismatic crystals, flattened on {010} and up to 0.5 mm diameter. Both spherulites and aggregates occur in interstices in arfvedsonite and microcline, in intimate association with golden-green tundrite-(Ce). Kihlmanite-(Ce) is brown, with a vitreous lustre and a pale yellowish-brown streak. The cleavage is perfect on {010}, parting is perpendicular to **c** and the fracture is stepped. Mohs hardness is ~3. In transmitted light, the mineral is yellowish brown; pleochroism and dispersion were not observed. Kihlmanite-(Ce) is biaxial (+), α = 1.708(5), β = 1.76(1), γ = 1.82(1) (589 nm), $2V_{calc}$ = 89°. The optical orientation is $Y \wedge c$ = 5°, other details are unclear. The calculated and measured densities are 3.694 and 3.66(2) g cm^{-3}, respectively. The mean chemical composition, determined by electron microprobe, is: Na_2O 0.13, Al_2O_3 0.24, SiO_2 9.91, CaO 1.50, TiO_2 11.04, MnO 0.26, Fe_2O_3 0.05, Nb_2O_5 2.79, La_2O_3 12.95, Ce_2O_3 27.33, Pr_2O_3 2.45, Nd_2O_3 8.12, Sm_2O_3 1.67, Gd_2O_3 0.49 wt.%, with CO_2 15.0 and H_2O 6.0 wt.% (determined by wet chemical and Penfield methods, respectively), giving a total of 99.93 wt.%. The empirical formula calculated on the basis of Si + Al = 1 atom per formula unit is $(Ca_{0.16}Na_{0.11}Mn_{0.02})_{\Sigma 0.29}[(Ce_{0.98}La_{0.47}Pr_{0.09}Nd_{0.29}Sm_{0.06}Gd_{0.02})_{\Sigma 1.91}(Ti_{0.82}Nb_{0.12})_{\Sigma 0.94}O_2(Si_{0.97}Al_{0.03})_{\Sigma 1}O_{4.02}(HCO_3)_{2.01}](H_2O)_{0.96}$. The simplified formula is $Ce_2TiO_2(SiO_4)(HCO_3)_2{\cdot}H_2O$. The mineral reacts slowly in cold 10% HCl with weak effervescence and fragmentation into separate plates. The strongest X-ray powder-diffraction lines [listed as d in Å (I) (hkl)] are as follows: 15.11(100)$(00\bar{1})$, 7.508(20)$(00\bar{2})$, 6.912(12)$(0\bar{1}1)$, 4.993(14)$(00\bar{3})$, 3.563(15)$(0\bar{2}1)$, 2.896(15)$(1\bar{2}\bar{2})$. The crystal structure

---

* E-mail: ivanyuk@ksc.ru

DOI: 10.1180/minmag.2014.078.3.01

of kihlmanite-(Ce) was refined to $R_1 = 0.069$ on the basis of 2441 unique observed reflections (Mo$K\alpha$, 293 K). It is closely related to the crystal structure of tundrite-(Ce) and is based upon $[Ce_2TiO_2(SiO_4)(HCO_3)_2]$ layers parallel to (001). Kihlmanite-(Ce) can be considered as a cation-deficient analogue of tundrite-(Ce). The mineral is named in honour of Alfred Oswald Kihlman (1858–1938), a remarkable Finnish geographer and botanist who participated in the Wilhelm Ramsay expeditions to the Khibiny Mountains in 1891–1892. The mineral name also reflects its occurrence at the Kihlman (Chil'man) Mountain.

KEYWORDS: kihlmanite-(Ce), new mineral, tundrite, crystal structure, alkaline pegmatite, Khibiny massif, Kola Peninsula.

Introduction

THE alkaline massifs of the Kola Peninsula are one of the world's leading localities for mineralogical diversity and complexity. More than 650 mineral species have been found there with >200 being discovered for the first time. Mineralogical studies of the alkaline massifs in this region started in the 19th century with the Wilhelm Ramsay expeditions in the Khibiny and Lovozero mountains (Brotherus *et al.*, 1890/92–94). A large number of the new minerals discovered in Kola are zircono-, niobo- and titanosilicates. Many factors contribute to their structural and chemical diversity, including natural cation exchange, decationization and protonation. Specific examples include the zirsinalite–lovozerite, kapustinite–litvinskite, kazakovite–tisinalite, lintisite–eliseevite–punkaruaivite and ivanyukite-Na-*T*–ivanyukite-Na-*C*–ivanyukite-K series (Pekov *et al.*, 2009; Yakovenchuk *et al.*, 2009, 2010, 2011). The most common mechanism in these series is $Na^+ \rightarrow H^+$ substitution: $Na^+ \rightarrow H_3O^+$ or $Na^+ + O^{2-} \rightarrow \square + (OH)^-$.

Kihlmanite-(Ce) is a cation-deficient analogue of tundrite-(Ce), $Na_2Ce_2TiO_2(SiO_4)(CO_3)_2$, a rare heterophyllosilicate discovered in the Lovozero alkaline massif by Semenov (1963). Tundrite-(Ce) was later described by Shlyukova *et al.* (1973) in alkaline pegmatites within fenitized metavolcanic rocks at the foot of the Kihlman Mountain in the Khibiny massif, the same locality as kihlmanite-(Ce). The mountain was named in honour of Alfred Oswald Kihlman (Kairamo) (1858–1938), a remarkable Finnish geographer and botanist and one of the members of the Wilhelm Ramsay expeditions (Brotherus *et al.*, 1890/92–94). Kihlmanite-(Ce) is named after the type locality as well as in honour of A. O. Kihlman.

Both mineral and mineral name have been approved by the Commission on New Minerals, Nomenclature and Classification of the International Mineralogical Association (IMA 2012–081). Type material is deposited in the collections of the Mineralogical Museum of St Petersburg State University, Russia, under catalogue number 1/19598 and in the Geological and Mineralogical Museum of the Geological Institute of the Kola Science Centre, Apatity, Russia, under catalogue number GIM 6790.

Occurrence

The Khibiny massif of nepheline syenites and foidolites is the world's largest alkaline complex occupying an area of ~1327 km^2 in the western Kola Peninsula, at the contact of the Imandra-Varzuga Proterozoic greenstone belt and the Archaean metamorphic complexes of the Kola–Norwegian megablock (Fig. 1). According to Pb-Pb, Rb-Sr and Sm-Nd dating (Arzamastsev *et al.*, 2007), the age of the main rock types of the Khibiny massif is 380–360 Ma.

The Imandra-Varzuga Proterozoic sedimentary volcanogenic complex consists mainly of greenschist-facies actinolite schists. Despite the gigantic size of the Khibiny massif, it is surrounded by a relatively narrow halo of metasomatic alteration. During the fenitization, actinolite is replaced by hornblende, which is in turn resorbed by the Na-rich diopside; carbonates and epidote disappear; the Na/Ca ratio in the plagioclase decreases; and, in some places, the rocks acquire a hornfelsic texture. At a distance of 50–80 m from the Khibiny massif, amphibolites are entirely transformed into diopside-andesine hornfels, a dark-grey rock with a greenish hue, fine grained and faintly schistose, with porphyroblasts of phlogopite, amphibole and microcline in places (Gorstka, 1971). Within the fenites, there are numerous alkaline pegmatites (Shlyukova *et al.*, 1973), of which one provides the type locality for kihlmanite-(Ce).

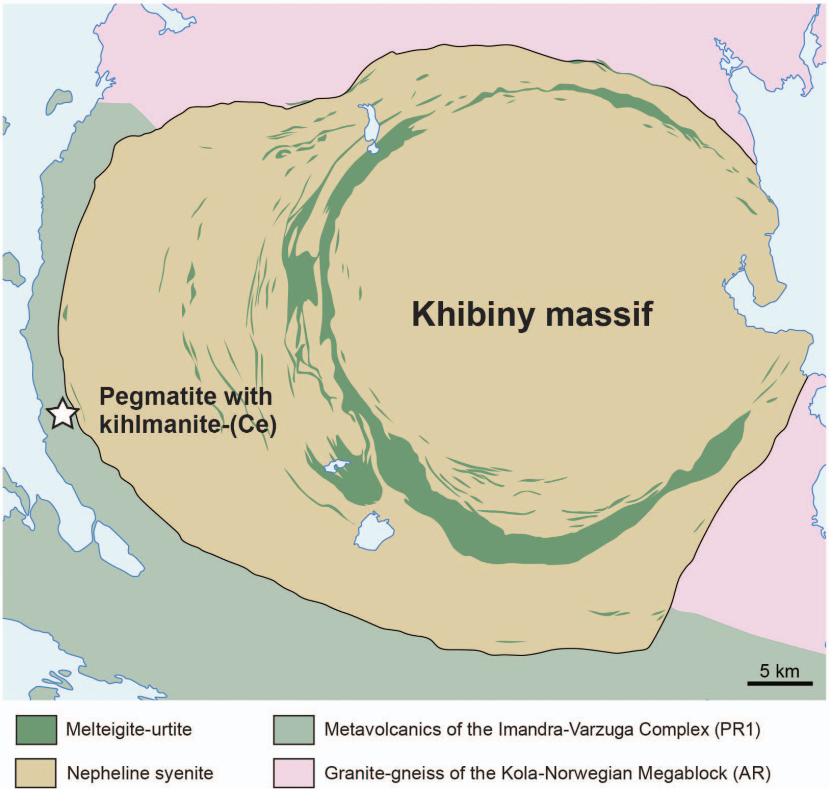

FIG. 1. Geological position of the kihlmanite-(Ce)-bearing pegmatite (67°41′32″, 33°14′19″E) relative to the Khibiny massif.

The kihlmanite-(Ce)-containing pegmatite (Fig. 2) is a large, symmetrically-zoned vein, varying from 0.5–2 m wide and measuring 280 m along the strike of 310–320° (Kostyleva-Labuntsova *et al.*, 1978; Yakovenchuk *et al.*, 2005). The vein has distinct contacts with the host fenitized metavolcanic rock. The fenite along the contact with the vein contains flattened prismatic rinkite and lens-shaped segregations of albite, aegirine, lamprophyllite, eudialyte and fluorapatite, crystals of which are elongated parallel to the vein extension.

The vein selvages are ~25 cm wide and are composed of acicular arfvedsonite with a small quantity of albite, eudialyte, lamprophyllite and astrophyllite. Intermediate zones (30–70 cm) are composed of aggregates of fine-grained albite, black acicular aegirine and ochre-brown rinkite. In some parts of the vein, there are granular segregations of natrolite and willemite (up to 2 cm diameter), colourless elongated grains of fluorapatite (up to 1 cm long), isometric crystals of lorenzenite, acicular vinogradovite, small purple and green grains of fluorite, pale-yellow grains of ancylite-(Ce), twinned cubo-octahedral crystals of loparite-(Ce), radiating aggregates (up to 2 cm diameter) of golden-green tundrite-(Ce) and reddish-brown kihlmanite-(Ce). In places, kihlmanite-(Ce) forms close intergrowths with tundrite-(Ce); the latter can be distinguished by its golden-green colour (Fig. 3). The axial zone (0.8–1.2 m) is composed of large tabular crystals of microcline (up to 12 cm diameter), with interstitial massive nepheline and sodalite, radiating aggregates of aegirine and twinned crystals of loparite-(Ce), flattened prismatic rinkite, rounded grains of eudialyte and aenigmatite, black prismatic crystals of arfvedsonite and anhedral grains of sphalerite and galena.

Both tundrite-(Ce) and kihlmanite-(Ce) are products of low-temperature hydrothermal alteration of rinkite and loparite-(Ce) and frequently occur in intergrowths. There is no direct evidence that kihlmanite-(Ce) is an alteration product of tundrite-(Ce).

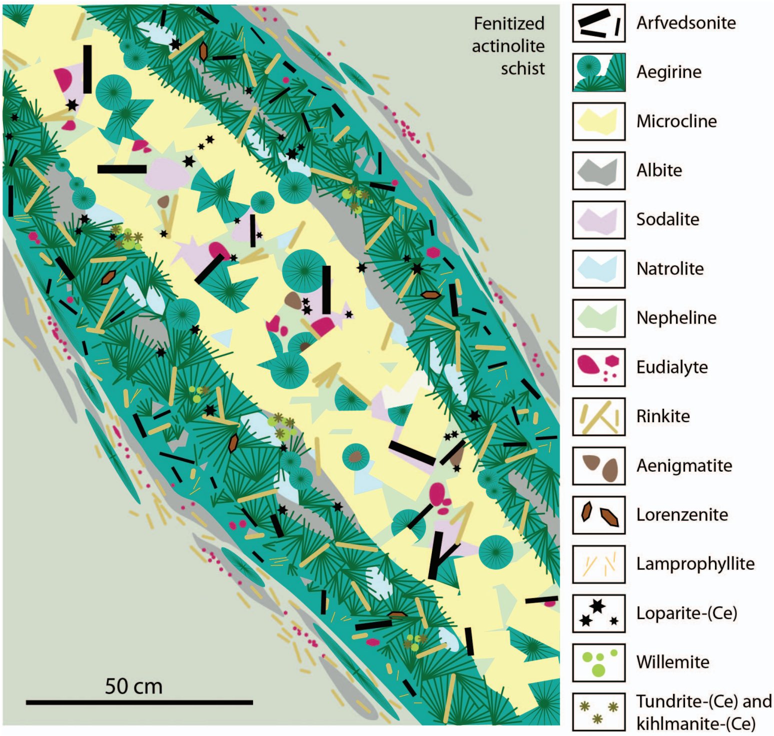

FIG. 2. Arfvedsonite-aegirine-microcline vein in fenitized metavolcanic rock at Mt Kihlman.

Morphology, physical and optical properties

Kihlmanite-(Ce) occurs as brown spherulites (up to 2 cm diameter) and sheaf-like aggregates of prismatic crystals up to 0.5 mm diameter, elongated along [001] and flattened on {010}. The {010}, {100}, {001}, {110} and {011} forms are common. The *a*:*b*:*c* ratio calculated from the unit-cell parameters is 0.662:1:2.053 (powder data) and 0.665:1:2.045 (single-crystal data). No twinning was observed. Cleavage is perfect on (010); parting is perpendicular to [001]. The mineral is brittle and has a stepped fracture. The Mohs hardness is ~3. The density, determined by the float-sink method in Clerici solution, is 3.66(2) g cm^{-3}. This value is in good agreement with the calculated density of 3.687 g cm^{-3} (using the empirical formula and powder unit-cell parameters) and 3.694 g cm^{-3} (using the empirical formula and single-crystal unit-cell parameters), but it is distinctly lower than the measured density of co-existing tundrite-(Ce): 3.78–3.82 g cm^{-3}.

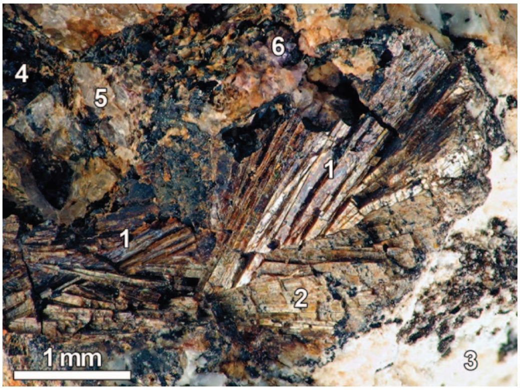

FIG. 3. Intergrowth of (1) kihlmanite-(Ce) and (2) tundrite-(Ce) in an aggregate of (3) microcline, (4) arfvedsonite, (5) willemite and (6) fluorite.

Macroscopically, kihlmanite-(Ce) is brown and has a vitreous lustre (silky in aggregates). The mineral is transparent, with a pale yellowish-brown streak. It is biaxial positive, with the refractive indices: α = 1.708(5), β =

TABLE 1. Chemical composition of kihlmanite-(Ce) and co-existing tundrite-(Ce) from Mt. Kihlman.

	1*	2	3	4	5	6	7	8
Na_2O, wt.%	0.13±0.85	0.37	0.86	2.41	3.56	4.70	4.82	4.97
Al_2O_3	0.24±0.17	–	–	–	–	–	–	–
SiO_2	9.91±1.10	11.11	12.15	9.57	9.66	9.73	9.68	9.88
K_2O	–	–	–	1.05	–	–	–	–
CaO	1.50±0.38	1.16	0.88	0.63	1.19	1.01	0.47	1.34
TiO_2	11.04±1.28	11.85	11.51	11.98	11.26	11.71	11.91	11.60
MnO	0.26±0.26	0.43	0.70	–	0.07	0.08	–	0.00
Fe_2O_3	0.05±0.03	–	0.07	–	–	–	–	–
ZnO	–	0.43	–	–	–	–	–	–
Nb_2O_5	2.79±0.85	2.93	2.33	0.81	2.69	1.97	0.94	2.58
La_2O_3	12.95±3.25	7.54	7.49	9.82	9.52	9.47	11.74	10.68
Ce_2O_3	27.33±1.41	25.40	25.37	27.92	25.27	25.83	26.85	25.99
Pr_2O_3	2.45±0.55	2.89	2.51	3.04	1.99	2.11	2.74	1.85
Nd_2O_3	8.12±0.97	10.44	10.29	8.93	9.45	9.55	9.47	8.00
Sm_2O_3	1.67±0.19	1.81	1.95	1.43	2.11	1.50	1.08	1.31
Eu_2O_3	–	0.51	0.73	–	–	–	–	–
Gd_2O_3	0.49±0.58	1.45	1.18	1.05	–	–	0.37	–
Dy_2O_3	–	0.66	0.43	–	–	–	–	–
CO_2	15.00							
H_2O	6.00							
Total	99.93	78.98	78.45	78.64	76.77	77.66	80.07	78.20
Na (a.p.f.u.)	0.11	0.07	0.14	0.49	0.72	0.94	0.97	0.98
K				0.14				
Ca	0.16	0.11	0.08	0.07	0.13	0.11	0.05	0.15
Mn	0.02	0.03	0.05		0.01	0.01		
Zn		0.03						
La	0.47	0.25	0.23	0.38	0.36	0.36	0.45	0.40
Ce	0.98	0.84	0.76	1.07	0.96	0.97	1.02	0.96
Pr	0.09	0.10	0.08	0.12	0.08	0.08	0.10	0.07
Nd	0.29	0.34	0.30	0.33	0.35	0.35	0.35	0.29
Sm	0.06	0.06	0.06	0.05	0.08	0.05	0.04	0.05
Eu		0.02	0.02					
Gd	0.02	0.04	0.03	0.04			0.01	
Dy		0.02	0.01					
Ti	0.82	0.80	0.71	0.94	0.88	0.91	0.93	0.88
Nb	0.12	0.12	0.09	0.04	0.13	0.09	0.04	0.12
Si	0.97	1.00	1.00	1.00	1.00	1.00	1.00	1.00
Al	0.03							
C	2.01							
H	3.93							
$\Sigma_{cations}$	13.01							

* holotype specimen of kihlmanite-(Ce). The proportions of cations are calculated on the basis of Si + Al = 1 a.p.f.u.

1.76(1), γ = 1.82(1) (589 nm), $2V_{calc}$ = 89(5)°. The optical orientation is $Y \wedge c$ = 5°, other details are unclear (they could not be determined because of the dark colour of the crystals). In transmitted light, the mineral is yellowish brown, without dispersion and pleochroism. The mineral is not fluorescent. A Gladstone-Dale calculation provides a compatibility index of −0.014, which is regarded as superior (Mandarino, 1981).

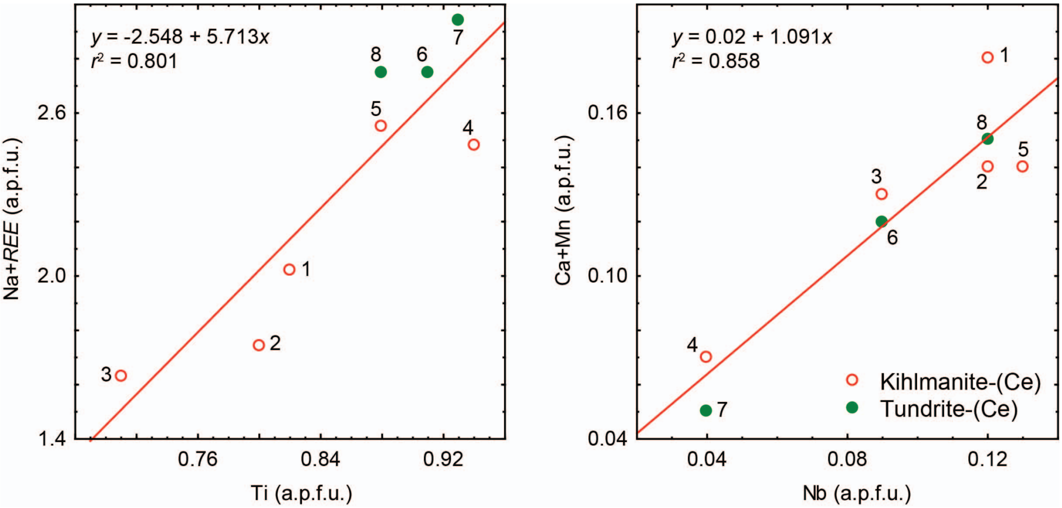

FIG. 4. The relations between the concentration of different chemical elements in kihlmanite-(Ce) (open circles) and tundrite-(Ce) (green circles).

Chemical composition

The chemical compositions of kihlmanite-(Ce) and co-existing tundrite-(Ce) were determined by wavelength-dispersive spectrometry using a Cameca MS-46 electron microprobe (at the Geological Institute, Kola Science Centre, Russian Academy of Sciences, Apatity) operating at 20 kV, 20–30 nA, with a 10 μm beam diameter. The standards used were: lorenzenite (Na, Ti), pyrope (Al), diopside (Si), fluorapatite (Ca), synthetic $MnCO_3$ (Mn), hematite (Fe), synthetic ZnO (Zn), metallic niobium (Nb), synthetic $LaCeS_2$ (La, Ce), synthetic $LiPr(WO_4)_2$ (Pr), synthetic $LiNd(MoO_4)_2$ (Nd), synthetic $LiSm(MoO_4)_2$ (Sm), synthetic $LiEu(MoO_4)_2$ (Eu), synthetic $LiGd(MoO_4)_2$ (Gd) and synthetic $LiDy(WO_4)_2$ (Dy). The H_2O and CO_2 contents were determined by the Penfield method (Sandell, 1951) and wet chemical methods on purified material, respectively. Table 1 provides the mean analytical results for eight different specimens of kihlmanite-(Ce) and tundrite-(Ce) including the holotype (the composition of each specimen is the mean of 2–8 different crystals for which the compositions are averages of the data obtained at five or six points

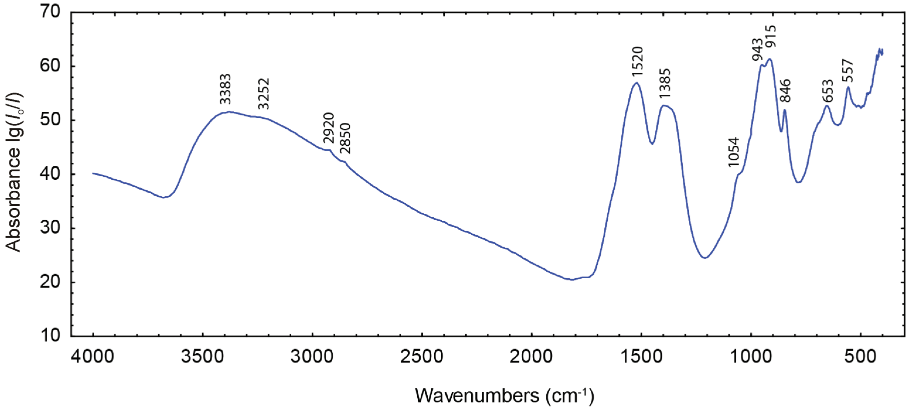

FIG. 5. Infrared absorption spectrum for kihlmanite-(Ce).

on each crystal). The crystals are, in general, chemically homogeneous, with slight variations in the Na and Ca contents.

The empirical formula of the holotype kihlmanite-(Ce) can be written as $(Ca_{0.16}Na_{0.11}Mn_{0.02})_{\Sigma 0.29}[(Ce_{0.98}La_{0.47}Pr_{0.09}Nd_{0.29}Sm_{0.06}Gd_{0.02})_{\Sigma 1.91}(Ti_{0.82}Nb_{0.12})_{\Sigma 0.94}O_2(Si_{0.97}Al_{0.03})_{\Sigma 1}O_{4.02}(HCO_3)_{2.01}](H_2O)_{0.96}$ {based on Si+Al = 1 atoms per formula unit (a.p.f.u.) } or $(Ca_{0.16}Na_{0.03}Mn_{0.02})_{\Sigma 0.21}[(Ce_{0.99}La_{0.47}Pr_{0.09}Nd_{0.29}Sm_{0.06}Gd_{0.02})_{\Sigma 1.92}(Ti_{0.82}Nb_{0.12})_{\Sigma 0.94}O_2(Si_{0.98}Al_{0.03})_{\Sigma 1.01}O_4(HC_{1.01}O_3)_2](H_{1.94}O)$ {based on O = 13 a.p.f.u.} by taking into account the results of the single-crystal X-ray diffraction study and infrared (IR) spectroscopy. The simplified formula is $Ce_2TiO_2(SiO_4)(HCO_3)_2{\cdot}H_2O$.

Statistical analysis of the data given in Table 1 shows that about half of the specimens studied have a sum of alkali metal and alkaline earth cations exceeding 0.50 a.p.f.u. According to the '50% rule', such species must be regarded as tundrite-(Ce) and the single-crystal X-ray diffraction study confirms their structural identity with tundrite-(Ce) from Mont Saint-Hilaire (Grice *et al.*, 2008). The compositions of both minerals depend linearly on substitution of Mn, Ca and Nb for Na, *REE* and Ti (Fig. 4) according to the following equation: $2Na^+ + REE^{3+} + Ti^{4+} \leftrightarrow \square(Ca,Mn)^{2+} + (Ca,Mn)^{2+} + Nb^{5+}$. However, this substitution cannot compensate for the deficit of Na in kihlmanite-(Ce). This is achieved by the protonation of carbonate groups according to the equation: $Na^+ + CO_3^{2-} \leftrightarrow \square + HCO_3^-$.

Reaction of kihlmanite-(Ce) grains with 1 M HCl (pH ≈ 1.5) resulted in their weak effervescence, fragmentation into separate plates and the appearance of silica gel clouds. The residual powder is amorphous.

Infrared spectroscopy

The IR spectrum of kihlmanite-(Ce) (Fig. 5) was obtained using a Nicolet 6700 Fourier-transform

TABLE 2. Crystal data, data collection and structure refinement parameters for kihlmanite-(Ce).

Crystal data	
Temperature	293 K
Radiation, wavelength	MoK_a, 0.71073 Å
Crystal system	triclinic
Space group	$P\bar{1}$
Unit-cell dimensions *a*, *b*, *c* (Å)	5.009(5), 7.533(5), 15.407(5)
α, β, γ (°)	103.061(5), 91.006(5), 109.285(5)
Unit-cell volume (Å^3)	531.8(7)
Z	2
Calculated density (g/cm^3)	3.694
Absorption coefficient (mm^{-1})	5.177
Crystal size (mm)	0.18 × 0.16 × 0.06
Data collection	
θ range	2.94–27.61°
h, *k*, *l* ranges	$-6 \rightarrow 6$, $-9 \rightarrow 9$, $-19 \rightarrow 20$
Total reflections collected	5715
Unique reflections (R_{int})	2441 (0.042)
Unique reflections $F > 4\sigma(F)$	1978
Structure refinement	
Refinement method	Full-matrix least-squares on F^2
Weighting coefficients *a*, *b*	0.0611, 34.4773
Extinction coefficient	0.0094(24)
Data/restraints/parameters	2441/0/191
R_1 [$F > 4\sigma(F)$], wR_2 [$F > 4\sigma(F)$],	0.069, 0.157
R_1 all, wR_2 all	0.086, 0.167
Goodness-of-fit on F^2	1.016
Largest diff. peak and hole, e Å^{-3}	2.74, −2.91

IR spectrometer using a KBr pellet. It is similar to that of tundrite-(Ce) (Grice *et al.*, 2008) but is simpler in the region of the Si−O vibrations between 400 and 950 cm^{-1} and has more intensive bands of O−H stretching vibrations at 3380, 2850 and 2920 cm^{-1}. Most of the bands can be interpreted by comparison of the IR spectrum of kihlmanite-(Ce) with spectra of other (hydro)-carbonates (White, 1971; Farmer and White, 1974; Grice *et al.*, 2008; Frost and Palmer, 2010). A medium-strong shoulder at 1620 cm^{-1} corresponds to the bending vibrations of H_2O molecules, whereas specific bands of hydroxyl vibrations at 3400−3600 cm^{-1} are not observed. Strong bands at 1520 and 1385 cm^{-1} can be assigned to asymmetric stretching vibrations of the $[CO_3]^{2-}$ or $[HCO_3]^-$ groups, whereas medium to strong bands at 1054 and 1020 cm^{-1} may be assigned to symmetric stretching vibrations of the $[HCO_3]^-$ groups. The strong bands at 653 and 700 cm^{-1} are probably caused by in-plane bending vibrations of the $[CO_3]^{2-}$ or $[HCO_3]^-$ groups. The weak peak at 1780 cm^{-1} can be considered as the sum of asymmetric stretching vibrations of the $[CO_3]^{2-}$ groups. Isolated $[SiO_4]^{4-}$ groups induce symmetric stretching vibrations at 846−943 cm^{-1} and bending vibrations at 557 cm^{-1}.

Crystal structure

Experimental

The crystal of kihlmanite-(Ce) selected for data collection was mounted on a Bruker APEX CCD diffractometer operated at 50 kV and 40 mA. More than a hemisphere of three-dimensional data were collected using Mo*K*α radiation and frame widths of 0.5º in ω, with 60 s used to acquire each frame. The unit-cell dimensions were refined on the basis of 1554 reflections (Table 2). The data were reduced using the Bruker program *SAINT*. A multi-scan absorption correction was applied and the data were corrected for Lorentz, polarization and background effects.

The Bruker *SHELXTL* system of programs was used for the solution and refinement of the crystal structure on the basis of F^2. The structure was

TABLE 3. Atom coordinates, site-occupation factors (SOFs) and equivalent isotropic displacement parameters (Å^2) in the structure of kihlmanite-(Ce).

Atom	SOF	*x*	*y*	*z*	U_{iso}
Ce1	$Ce_{0.973(7)}$	0.2288(3)	0.38821(13)	0.19835(7)	0.0223(4)
Ce2	$Ce_{0.966(9)}$	−0.0536(4)	−0.17637(15)	0.19757(8)	0.0241(5)
Ti	$Ti_{0.76(2)}Nb_{0.24(2)}$	0.3073(4)	0.6148(3)	0.99972(15)	0.0176(8)
Si	Si	0.5023(8)	0.0684(6)	0.1289(3)	0.0178(8)
O1	O	0.282(2)	−0.1476(13)	0.0759(7)	0.015(2)
O2	O	0.467(2)	0.2281(13)	0.0762(7)	0.015(2)
O3	O	0.351(2)	0.1174(15)	0.2207(8)	0.022(2)
O4	O	−0.050(2)	0.5288(13)	0.9250(6)	0.014(2)
O5	O	0.615(2)	0.6098(13)	0.0747(7)	0.015(2)
O6	O	0.823(2)	0.0764(15)	0.1475(8)	0.024(2)
O7	O	−0.213(3)	−0.4933(17)	0.2369(8)	0.030(3)
O8	O	0.402(3)	0.7438(16)	1.2395(9)	0.033(3)
O9	O	−0.429(4)	−0.516(2)	1.3591(11)	0.057(4)
O10	O	−0.008(4)	−0.575(3)	1.3441(12)	0.065(5)
O11	O	0.271(6)	0.894(3)	1.3593(14)	0.088(7)
O12	O	0.769(6)	0.945(3)	1.3429(14)	0.090(7)
C1	C	−0.218(4)	−0.524(3)	1.3181(14)	0.042(5)
C2	C	0.494(6)	0.866(3)	1.3193(18)	0.055(6)
Ca1	$Ca_{0.22(4)}$	0.312(3)	0.489(2)	1.4839(8)	0.015(5)
Ca2	$Ca_{0.18(4)}$	0	0	0	0.033(10)
H_2O1	$H_2O_{0.52(4)}$	0.304(4)	0.583(4)	1.4924(13)	0.038(8)
H_2O2	$H_2O_{0.32(7)}$	0	0	½	0.04(2)
Q1	$Ce_{0.027(7)}$	0.342(10)	0.370(4)	0.2025(18)	0.007(11)
Q2	$Ce_{0.034(9)}$	0.046(12)	−0.197(5)	0.206(2)	0.021(11)

solved by direct methods. The occupancies of the cation positions were refined from the experimental site-scattering factors in accordance with the empirical chemical composition. Hydrogen sites could not be located. Refinement of all atom-position parameters, allowing for the anisotropic displacement of all atoms except partially occupied sites and the inclusion of a refinable weighting scheme for the structure factors, resulted in a final agreement index (*R*1) of 0.069, calculated for the 2441 observed unique reflections ($|F_o| > 4\sigma F$) and a goodness-of-fit (*S*) of 1.016. The final atom parameters are in Table 3 and selected interatomic distances in Table 4.

Results

The structure of kihlmanite-(Ce) is closely related to that of tundrite-(Ce) (Shumyatskaya *et al.*, 1969, 1976; Grice *et al.*, 2008). It contains two nine-coordinated Ce sites with Ce–O distances in the range 2.377–2.800 Å (Fig. 6). Close to the main Ce sites, two ghost peaks were observed, Q1 and Q2, located at 0.63(6) and 0.59(7) Å from the Ce1 and Ce2 sites, respectively. If occupancies of these sites are refined using Ce site-scattering functions, they appear to be very low [0.027(7) and 0.034(9), respectively]. Similarly to the Ce1 and Ce2 sites, the *Q1* and *Q2* sites are nine-coordinated, but display a strong deviation of coordination with the *Q*–O bond lengths in the range of 1.92–3.30 Å. The appearance of these peaks cannot be explained but one suggestion is that they may be the result of the presence of Ce^{4+} cations partially substituting the Ce^{3+} cations at the Ce sites. Another possible explanation is that the ghost peaks are due to the admixture of tundrite slabs in the studied crystal, which provide extra electron density close to the Ce positions.

TABLE 4. Selected bond lengths (Å) in the structure of kihlmanite-(Ce).

Ce1–O4	2.377(9)	Ce2–O5	2.384(10)
Ce1–O3	2.407(11)	Ce2–O3	2.406(11)
Ce1–O8	2.451(12)	Ce2–O6	2.456(11)
Ce1–O6	2.495(11)	Ce2–O7	2.473(12)
Ce1–O2	2.536(10)	Ce2–O12	2.51(2)
Ce1–O10	2.56(2)	Ce2–O1	2.539(10)
Ce1–O7	2.651(13)	Ce2–O8	2.647(13)
Ce1–O7	2.674(13)	Ce2–O8	2.716(14)
Ce1–O9	2.795(18)	Ce2–O11	2.80(2)
<Ce1–O>	2.550	<Ce2–O>	2.549
Ti–O5	1.925(9)	C1–O9	1.25(3)
Ti–O4	1.943(10)	C1–O7	1.32(2)
Ti–O1	1.949(10)	C1–O10	1.32(3)
Ti–O2	1.958(10)	<C1–O>	1.30
Ti–O4	1.969(9)		
Ti–O5	1.976(9)	C2–O12	1.31(3)
<Ti–O>	1.953	C2–O8	1.33(3)
		C2–O11	1.34(3)
Na1–H_2O1	2.21(3)	<C2–O>	1.33
Na1–O9	2.34(2)		
Na1–O9	2.43(2)	Si–O6	1.604(11)
Na1–O10	2.52(2)	Si–O3	1.642(12)
Na1–H_2O1	2.99(2)	Si–O2	1.647(10)
Na1–O10	3.13(2)	Si–O1	1.647(10)
<Na1–O>	2.60	<Si–O>	1.635
Na2–O6	2.470(12) 2 ×		
Na2–O2	2.479(10) 2 ×		
Na2–O1	2.485(10) 2 ×		
<Na2–O>	2.478		

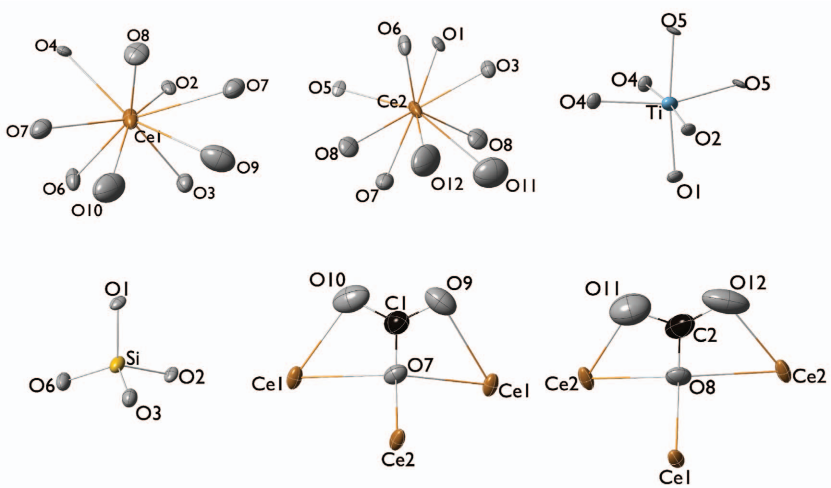

FIG. 6. Coordination of cations in the structure of kihlmanite-(Ce). Displacement ellipsoids are drawn at the 50% probability level.

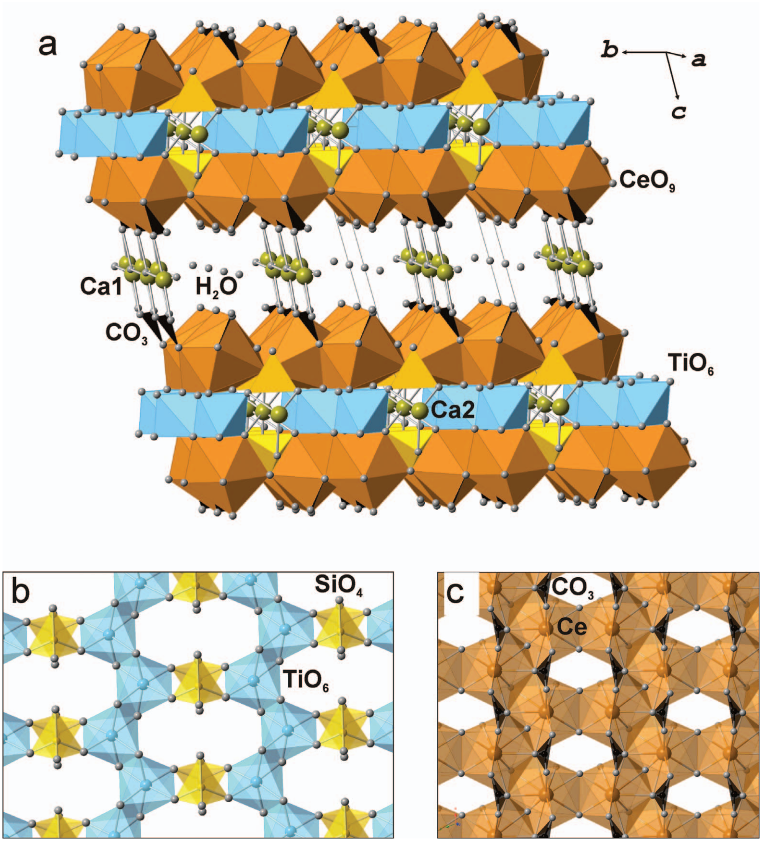

FIG. 7. (*a*) Projection of the crystal structure of kihlmanite-(Ce), (*b*) Structure of titanosilicate and (*c*) Ce–CO_3 layers.

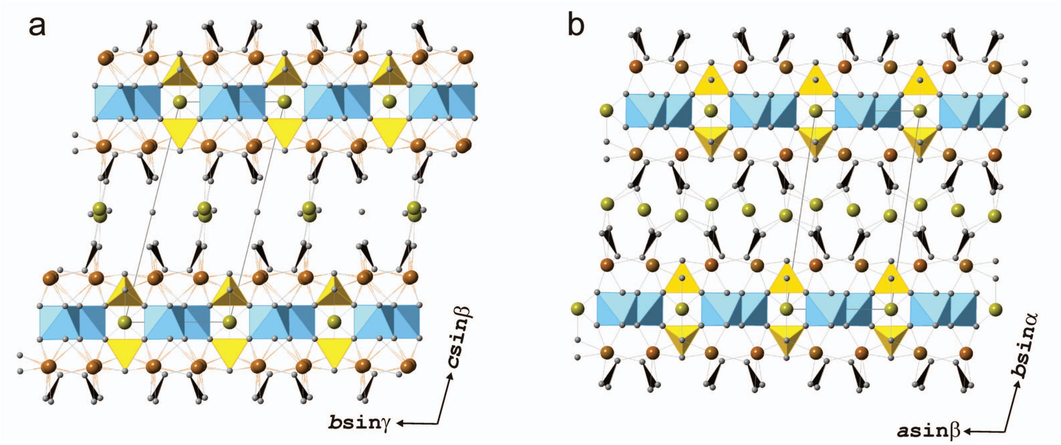

FIG. 8. The crystal structures of (*a*) kihlmanite-(Ce) and (*b*) tundrite-(Ce) projected along the *a* and *c* axes, respectively. Legend as in Fig. 7.

One Ti site is octahedrally coordinated to six O atoms. There are two symmetrically independent HCO_3 groups each coordinated by three adjacent Ce atoms. Each group has one O atom (O7 for $C1O_3$ and O8 for $C2O_3$) bonded to two Ce atoms; the respective C−O bond is elongated (C1−O7 = 1.32 Å and C2−O8 = 1.33 Å). Two other O atoms of each group are coordinated by one Ce atom only and the respective C−O distances are in the range of 1.25−1.34 Å. Taking into account the presence of the HCO_3^- groups in kihlmanite-(Ce) detected by IR spectroscopy, protonation is assumed to occur in a statistical fashion to the mono-coordinated O atoms of the carbonate groups (i.e. to the O9−O12 sites).

There are two Ca sites in the structure of kihlmanite-(Ce). The Ca1 site is located in the interlayer and is only 25% occupied. The Ca2 site is in between the chains of TiO_6 octahedra and has 20% occupancy. Both sites are each coordinated by six O atoms.

The structure of kihlmanite-(Ce) is based upon complex $[Ce_2TiO_2(SiO_4)(HCO_3)_2]$ layers parallel to (001) (Fig. 7*a*). The layers consist of chains of edge-sharing TiO_6 octahedra interlinked by isolated SiO_4 tetrahedra (Fig. 7*b*). The Ce^{3+} cations are located on both sides of the layers and are further coordinated by HCO_3^- anions (Fig. 7*c*). There are two Ca sites with less occupancy. The Ca1 site is located in the interlayer space, whereas the Ca2 is inside the layers, directly between the chains of TiO_6 octahedra. The structure of tundrite-(Ce) is based upon structurally identical layers (Fig. 8*b*), but

TABLE 5. X-ray powder diffraction data for kihlmanite-(Ce).

I_{rel}	d_{obs} (Å)	d_{calc} (Å)	*hkl*
100	**15.11**	14.978	$00\bar{1}$
20	**7.508**	7.489	$00\bar{2}$
12	**6.912**	6.962	$0\bar{1}1$
2	5.851	5.859	$0\bar{1}2$
14	**4.993**	4.993	$00\bar{3}$
7	4.715	4.695	$1\bar{1}0$
4	4.134	4.120	$1\bar{1}2$
7	3.830	3.850	$1\bar{1}\bar{2}$
		3.816	1·0·2
15	**3.563**	3.560	$0\bar{2}1$
10	3.454	3.444	$11\bar{1}$
11	**3.198**	3.243	$0\bar{2}\bar{1}$
		3.187	$0\bar{2}3$
			$0\bar{2}\bar{1}$
12	**3.065**	3.064	$1\bar{2}3$
9	3.001	2.996	$00\bar{5}$
15	**2.896**	2.895	$1\bar{2}\bar{2}$
10	2.775	2.792	$11\bar{4}$
		2.766	$1\bar{2}4$
2	2.618	2.616	$1\bar{1}5$
9	2.491	2.497	$2\bar{1}0$
		2.496	$00\bar{6}$
7	2.362	2.362	$0\bar{3}1$
6	2.293	2.318	$0\bar{2}6$
1	2.133	2.140	$00\bar{7}$
6	2.048	2.047	$21\bar{1}$
4	1.965	1.963	2·1·1
6	1.911	1.909	$21\bar{4}$
7	1.886	1.887	$2\bar{3}\bar{2}$
		1.886	$13\bar{2}$
4	1.778	1.780	2·1·3

The eight strongest lines are listed in bold.

replacement of HCO_3 groups by CO_3 groups as well as different Ca and H_2O content results in considerable modification of the structure type. The difference between the two structures might be described in terms of mutual relationships between adjacent $[Ce_2TiO_2(SiO_4)(HCO_3/CO_3)_2]$ layers as follows (Fig. 8). The interlayer is considerably expanded in kihlmanite-(Ce); the distance between the layers is 13.57 Å in tundrite-(Ce) and 14.93 Å in kihlmanite-(Ce). In addition, the layers are shifted in kihlmanite-(Ce) relative to each other by ~1.9 Å in a direction perpendicular to the extension of titanate octahedral chains. These differences result in a distinctly different unit cell (see below).

The crystal-chemical formula of kihlmanite-(Ce) calculated on the basis of the crystal-structure refinement can be written as $Ca_{0.35}Ce_2(Ti_{0.76}Nb_{0.24})O_2(SiO_4)(HCO_3)_{1.06}(CO_3)_{0.94}(H_2O)_{0.84}$, which is, in general, in good agreement with the results of electron microprobe analysis, taking into account the possibility of Ca → Na substitution at the Ca sites.

X-ray powder diffraction

The X-ray powder diffraction pattern of kihlmanite-(Ce) was obtained using a STOE IPDS II instrument (in Gandolfi mode using Mo$K\alpha$ radiation) operating at 40 kV and 30 mA (Table 5). Refined unit-cell parameters are as follows: $a = 4.994(2)$, $b = 7.54(2)$, $c = 15.48(4)$ Å, $\alpha = 103.5(4)$, $\beta = 90.7(2)$, $\gamma = 109.2(2)^{\circ}$, with $V = 533(1)$ Å^3 and $Z = 2$, which are in good agreement with the single-crystal data (see Table 2).

Discussion

Kihlmanite-(Ce) is closely related to tundrite-(Ce) (Table 6), though it has distinctly different

TABLE 6. Comparative data for kihlmanite-(Ce) and tundrite-(Ce).

	Kihlmanite-(Ce)	Tundrite-(Ce)*
Formula	$[Ce_2TiO_2(SiO_4)(HCO_3)_2]\cdot H_2O$	$Na_2[Ce_2TiO_2(SiO_4)(CO_3)_2]$
Crystal system	Triclinic	Triclinic
Space group	$P\bar{1}$	$P\bar{1}$
a, b, c (Å)	5.01, 7.53, 15.41	7.56, 13.96, 5.04
α, β, γ (°)	103.1, 91.0, 109.3	101.1, 70.5, 100.0
Z	2	2
Strongest lines in powder pattern	15.11 (100)	3.99 (40)
	7.508 (20)	3.38 (30)
	6.912 (12)	3.03 (70)
	4.993 (14)	2.71 (100)
	3.563 (15)	1.77 (40)
	2.896 (15)	1.68 (40)
Density g/cm^3	3.66	4.09
Mohs hardness	~3	3
Colour	brown	olive-green
Opt. character	biaxial (+)	biaxial (+)
α	1.745	1.731-1.761
β	1.80	1.80
γ	1.88	1.90
2*V*°	89 (calc)	*ca* 90 (meas)
Orientation	$Y \wedge c = 5^{\circ}$	-
Dispersion	not observed	not observed
Pleochroism	not observed	distinct: on γ – greenish-yellow, on α – light-yellow
Habit	flattened on (010) long prismatic [001] crystals	flattened on (010) long prismatic [001] crystals
Cleavage	{010} perfect	{010} perfect
Parting	perpendicular to **c**	perpendicular to **c**

* Shlyukova *et al.* (1973); Kostyleva-Labuntsova *et al.* (1978).

properties and crystallographic parameters. Both these minerals are of hydrothermal origin and crystallized from solutions enriched in Ti and Ce that result from alteration of primary rinkite and/or loparite-(Ce). At first glance, kihlmanite-(Ce) itself could be regarded as a result of decationization and protonation of tundrite-(Ce) according to the following reaction:

$$Na_2Ce_2TiO_2(SiO_4)(CO_3)_2 + 3H_2O = Ce_2TiO_2(SiO_4)(HCO_3)_2{\cdot}H_2O + 2Na(OH)$$

However, treatment of tundrite-(Ce) and kihlmanite-(Ce) with a dilute solution of K and Cs chlorides (pH = 6.0–6.2) resulted in a leaching of 2–3 wt.% of silica, whereas the contents of *REE*, Ti and even Na remained intact. In acidic solutions (pH = 1–2), both these minerals transform rapidly into an amorphous powder. Therefore, there is no evidence to suggest that kihlmanite-(Ce) is the result of a natural transformation of tundrite-(Ce). These minerals co-exist in the same locality without any indication of a chemical transition, which also testifies against the transformation hypothesis. Most probably, tundrite-(Ce) was the first phase in the paragenetic sequence, whereas crystallization of kihlmanite-(Ce) started when the alkalinity of a hydrothermal solution decreased due to the precipitation of Na-rich minerals.

Acknowledgements

The authors are grateful to Uwe Kolitsch, Joel Grice and Ed Grew for useful and constructive comments on the manuscript. This work was supported by Presidium of Russian Academy of Science through Program No. 27, Project 1.2.4 and by the Russian Foundation for Basic Research through the grants 120598802 and 12-05-31190. SVK, AAZ and ESZ have been supported in this work by St. Petersburg State University internal grant 3.38.136.2014.

References

Arzamastsev, A.A., Arzamastseva, L.V., Travin, A.V., Belyatsky, B.V., Shamatrina, A.M., Antonov, A.V., Larionov, A.N., Rodionov, N.V. and Sergeev, S.A. (2007) Duration of formation of magmatic system of polyphase paleozoic alkaline complexes of the Central Kola: U–Pb, Rb–Sr, Ar–Ar data. *Doklady Earth Sciences*, **413(2)**, 432–436.

Brotherus, V.F., Kairamo, A.O., Palmén, J.A.F., Ramsay, W., Petrelius, A., Linden, J., Hackman, V.A., Sælan, T. and Sanio, C. (1890/92–94) *Wissenschaftliche Ergebnisse der Finnischen Expeditionen nach der Halbinsel Kola in den Jahren 1887–1892*. Backmans Druckerei, Kupio, Helsingfors [Helsinki].

Farmer, V.C. and White, W.B. (1974) Carbonate Minerals. Pp. 227–279 in: *The Infrared Spectra of Minerals* (V.C. Farmer, editor). Monograph **No. 4**. The Mineralogical Society, London.

Frost, R.L. and Palmer, S. J. (2010) Infrared and infrared emission spectroscopy of nesquehonite $Mg(OH)(HCO_3){\cdot}2H_2O$ – implications for the formula of nesquehonite. *Spectrochimica Acta. Part A: Molecular and Biomolecular Spectroscopy*, **78**, 1255–1260.

Gorstka, V.N. (1971) *Kontaktovaya Zona Khibinskogo Massiva (Contact Zone of the Khibiny Massif)*. Nauka, Leningrad, Russia, [in Russian].

Grice, J.D., Rowe, R., Poirier, G. and Wight, Q. (2008) Tundrite-(Ce) from Mont Saint-Hilaire, Quebec: crystal structure analysis and species characterization. *The Canadian Mineralogist*, **46**, 413–422.

Kostyleva-Labuntsova, E.E., Borutsky, B.E., Sokolova, M.N., Shlyukova, Z.V., Dorfman, M.D., Dudkin, O.B., Kozyreva, L.V. and Ikorsky, S.V. (1978) *Mineralogiya Khibinskogo Massiva (Mineralogy of the Khibiny massif). 2: Minerals*. Nauka, Moscow, [in Russian].

Mandarino, J.A. (1981) The Gladstone-Dale relationship: Part IV. The compatibility concept and its application. *The Canadian Mineralogist*, **19**, 441–450.

Pekov, I.V., Krivovichev, S.V., Zolotarev, A.A., Yakovenchuk, V.N., Armbruster, T. and Pakhomovsky, Ya.A. (2009) Crystal chemistry and nomenclature of the lovozerite group. *European Journal of Mineralogy*, **21**, 1061–1071.

Sandell, E.B. (1951) Micro determination of water by the Penfield method. *Microchimica Acta*, **38**, 487–491.

Semenov, E.I. (1963) *Mineralogiya Redkikh Zemel' (Mineralogy of the Rare Earths)*. Academy of Science of USSR, Moscow, [in Russian].

Shlyukova, Z.V., Vlasova, E.V., Kazakova, M.E., Piloyan, G.O., Shumyatskaya, N.G. and Borutsky, B.E. (1973) New data on tundrite. *Doklady Akademii Nauk SSSR*, **211**, 426–429, [in Russian].

Shumyatskaya, N.G., Ilyukhin, V.V., Voronkov, A.A. and Belov, N.V. (1969) Crystal structure of tundrite. *Doklady Akademii Nauk SSSR*, **185**, 1289–1292, [in Russian].

Shumyatskaya, N.G., Voronkov, A.A., Ilyukhin, V.V. and Belov, N.V. (1976) Tundrite, $Na_2Ce_2TiO_2(SiO_4)(CO_3)_2$, refinement of the crystal structure and chemical formula. *Kristallografiya*, **21**, 705–715, [in Russian].

White, W.B. (1971) Infrared characterization of water and hydroxyl ion in the basic magnesium carbonate minerals. *American Mineralogist*, **56**, 46–53.

Yakovenchuk, V.N., Ivanyuk, G.Y., Pakhomovsky, Y.A. and Men'shikov, Y.P. (2005) *Khibiny*. Laplandia Minerals, Apatity, Russia.

Yakovenchuk, V.N., Nikolaev, A.P., Selivanova, E.A., Pakhomovsky, Ya.A., Korchak, J.A., Spiridonova, D.V., Zalkind, O.A. and Krivovichev, S.V. (2009) Ivanyukite-Na-*T*, ivanyukite-Na-*C*, ivanyukite-K and ivanyukite-Cu: New microporous titanosilicates from the Khibiny massif (Kola Peninsula, Russia) and crystal structure of ivanyukite-Na-*T*. *American Mineralogist*, **94**, 1450–1458.

Yakovenchuk, V.N., Ivanyuk, G.Yu., Pakhomovsky, Y.A., Selivanova, E.A., Men'shikov,Yu.P., Korchak, J.A., Krivovichev, S.V., Spiridonova, D.V. and Zalkind, O.A. (2010) Punkaruaivite, $LiTi_2[Si_4O_{11}(OH)](OH)_2 \cdot H_2O$, a new mineral species from hydrothermal assemblages, Khibiny and Lovozero alkaline massifs, Kola peninsula, Russia. *The Canadian Mineralogist*, **48**, 41–50.

Yakovenchuk, V.N., Ivanyuk, G.Yu., Krivovichev, S.V., Pakhomovsky, Ya.A., Selivanova, E.A., Korchak, J.A., Men'shikov, Yu.P., Drogobuzhskaya, S.V. and Zalkind, O.A. (2011) Eliseevite, $Na_{1.5}Li[Ti_2Si_4O_{12.5}(OH)_{1.5}] \cdot 2H_2O$, a new microporous titanosilicate from the Lovozero alkaline massif (Kola Peninsula, Russia). *American Mineralogist*, **96**, 1624–1629.